Dalton Transactions

The Pressure-Stabilized Polymorph of Indium Triiodide

Journal:	*Dalton Transactions*
Manuscript ID	DT-COM-11-2023-003771.R1
Article Type:	Communication
Date Submitted by the Author:	04-Dec-2023
Complete List of Authors:	Ni, Danrui; Princeton University, Chemistry Wang, Haozhe; Michigan State University, Chemistry Xu, Xianghan; Princeton University, Chemistry Xie, Weiwei; Michigan State University, Chemistry Cava, Robert; Princeton University, Department of Chemistry

COMMUNICATION

The Pressure-Stabilized Polymorph of Indium Triiodide

Danrui Ni, [a] Haozhe Wang, [b] Xianghan Xu, [a] Weiwei Xie [b] and Robert J. Cava *[a]

Received 00th January 20xx,
Accepted 00th January 20xx

DOI: 10.1039/x0xx00000x

A layered rhombohedral polymorph of indium (III) triiodide is synthesized at high pressure and temperature. The unit cell symmetry and approximate dimensions are determined by single crystal X-ray diffraction. Its $R\bar{3}$ crystal structure, with a = 7.214 Å, and c = 20.47 Å, is refined by the Rietveld method on powder X-ray diffraction data. The crystal structure is based on InI_6 octahedra sharing edges to form honeycomb lattice layers, though with considerable stacking defects. Different from ambient pressure InI_3, which has a monoclinic molecular structure and a light-yellow color, high pressure InI_3 is layered and has an orange color. The band gaps of both the monoclinic and rhombohedral variants of InI_3 are estimated from diffuse reflectance measurements.

High pressure synthesis and the influence of high-pressure treatment have attracted researchers' attention in recent years, as the application of pressure can lead to significant changes in reaction equilibria and affect both the structures and physical properties of compounds[1–3]. High-pressure high-temperature synthetic techniques may introduce phase transitions and lead to different polymorphs[4–6], or result in new formulas or structures[7–9] that cannot be stabilized using traditional preparation methods at ambient pressure.

Metal trihalides often crystallize in crystal structures consisting of 1D-chains or 2D-honeycomb layers [10–12]. Polymorphism and phase transition behavior, as well as the structure-related properties of different phases, are aspects of their study [13–16], and pressure-induced polymorphism has been reported in several transition-metal-based systems[17–19]. In this context, some main-group-metal halide systems such as the indium iodide system[20] have also been reported to have relatively complex polymorphic behavior. Based on information in the Inorganic Crystal Structure Database, indium triiodide (InI_3) is suggested to have an aluminum triiodide type monoclinic structure with In_2I_6 dimers at ambient pressure[21]. Another InI_3 polymorph, mentioned in the literature as early as the 1940s[22] as a low-temperature phase, was suggested to be light-sensitive and isostructural to the low-temperature phase of $CrCl_3$[20], but no modern structural refinement results were reported. In this report, we describe an $R\bar{3}$polymorph of InI_3 with a honeycomb layered structure that is stabilized by high pressure synthesis. The structure was determined by powder X-ray diffraction (PXRD) via Rietveld refinement, with the space group symmetry and cell parameters qualitatively determined by single crystal X-day diffraction (SCXRD). Stacking faults occur in significant amounts in high pressure InI_3, which smear out the diffraction peaks (shown below), making single crystal structure refinements unreliable. Finally, some light absorption and physical properties are characterized.

Rhombohedral InI_3 was prepared using high-pressure synthesis method (HP-InI_3). The ambient-pressure phase of monoclinic InI_3 (AP-InI_3) was used as the starting material. Both materials are air-sensitive and hygroscopic. The purity of the AP-InI_3 starting material was confirmed by Le Bail fitting, as was its $P2_1/c$ monoclinic symmetry (Figure 1A and 1B), consistent with the reported structure[21]. Different from the light-yellow colored AP-InI_3 powder, the sample after high pressure reaction (HP-InI_3, shown in Figure 1C) appears to be orange after grinding (Figure 1B and 1D insets). Rietveld refinement of the PXRD data of HP-InI_3, collected at 300 K in an air-free environment (Figure 1D and Table 1), suggests that it has an $R\bar{3}$ space group (#148) with lattice parameters a = 7.2144(4) Å and a c = 20.4704(9) Å. Due to a significant amount of disorder and stacking errors, the refinement gives 73.3% of the total indium content located at the honeycomb site (6c Wyckoff site), and 26.7% at a site in the honeycomb hole (the 3a site). The rhombohedral unit cell contains three layers of honeycomb lattice material (Figure 1C), formed by edge-sharing InI_6 octahedra. The space group symmetry is confirmed by the single crystal diffraction data

[a] *Department of Chemistry, Princeton University, Princeton, NJ 08544, USA.*
[b] *Department of Chemistry, Michigan State University, East Lansing, MI 48824, USA.*

Electronic Supplementary Information (ESI) available: CCDC deposition number 2311271; The experimental methods and details; Selected bond lengths and bond angles information. See DOI: 10.1039/x0xx00000x

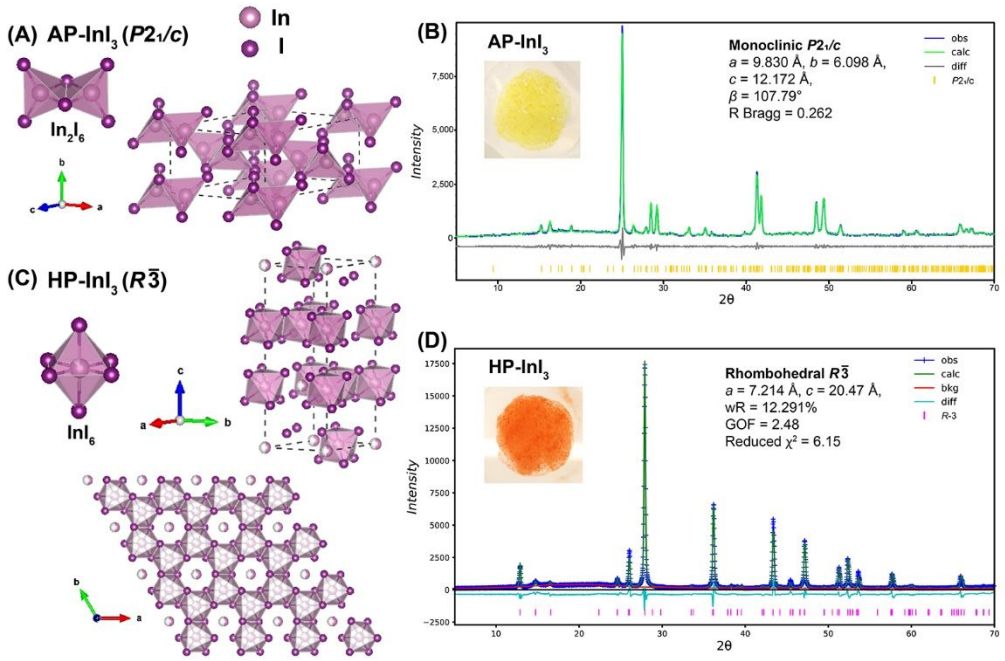

Figure 1 (A) Crystal structure of monoclinic AP-InI_3 with In_2I_6 dimer; (B) Le Bail fitting of PXRD pattern of AP-InI_3, with a photo of powder sample shown as inset; (C) Crystal structure of $R\bar{3}$ HP-InI_3, with a view through *c*-direction to reveal the in-plane honeycomb lattice, as well as the InI_6 coordination octahedron; (D) Rietveld refinement of HP-InI_3 PXRD pattern, with a photo of powder sample shown as the inset. The reflection positions are labeled with colored sticks in the powder diffraction patterns.

shown in Figure 2, especially in the (hk0) and (hk1) reciprocal lattice planes, although some ambiguous scattering may be observed due to the disorder in the system. (The streaking in the (h0l) and (0kl) reciprocal lattice planes is an indication of the disorder in the system.)

In HP-InI_3, the indium has a relatively symmetric octahedral coordination, with the In-I bond lengths ranging from 2.904 to 2.911 Å in the InI_6 octahedra (Table S1). When comparing these two polymorphs of InI_3, it is revealed that the In atoms in AP-InI_3, which display a tetrahedral coordination, bond to iodine with distances at around 2.64 Å (the bonds to the iodines forming the unshared edges of the dimers) and 2.84 Å (the bonds forming the shared edges of the dimers)[21]. These In-I bond lengths are generally shorter than the ones in HP-InI_3, which suggests a stronger In-I bonding in the In_2I_6 dimer of AP-InI_3. However, based on the structures presented in Figure 1, AP-InI_3 is closer to being a molecular solid, in other words a much weaker interaction between different dimer units is observed. This may be due to the influence of iodine lone pairs in the AP polymorph, leading to the significantly lower density of AP-InI_3 (4.72 g/cm^3) compared to HP-InI_3 (5.35 g/cm^3), thus making the $R\bar{3}$ polymorph more favored under pressure. This structural type, based on stacked honeycomb layers, is relatively common in metal trihalides[14]. Similar pressure-induced phase transition behavior can also be observed for $Mg(IO_3)_2$, which transits from a monoclinic $P2_1$ phase to a trigonal *P*3 between 7.5 and 9.7 GPa at ambient temperature[23]. It is consistent with the commonly held principle that high pressure favors phases with higher density and larger coordination number.

The unit cell and color of HP-InI_3 match the description of the "low-temperature polymorph" of InI_3 [20,24]. Although the latter paper is inclined to assign an *R*3 symmetry to that polymorph based on a Hamilton significance test, we have not found evidence for the absence of an inversion center when determining the structure of HP-InI_3 and thus attribute $R\bar{3}$ to the phase in this report. Previous reports also indicated that this phase is light-sensitive (while ours is not), and that it would

Table 1 Structural parameters and standardized crystallographic positions of HP-InI_3, from the Rietveld refinement of laboratory PXRD data collected at 300 K. wR = 12.29%, GOF = 2.479, reduced χ^2 = 6.15. Due to the multiplicity differences, the 6*c* site accounts for 73.3% of the In total while the 3*a* site accounts for 26.7%. (Standard deviations are indicated by the values in parentheses).

Refined Formula			**InI_3**				
F.W. (g/mol)			495.54				
Symmetry			Trigonal				
Space group; *Z*			$R\bar{3}$ (#148); 6				
a(Å)			7.2144(4)				
c(Å)			20.4704(9)				
V (Å^3)			922.69(9)				
Density (g/cm^3)			5.3508				
Atom	**Wyck.**	**Occ.**	***x***	***y***	***z***	**U_{iso} equiv. [Å^2]**	**Multi.**
I1	18*f*	1	0.3517(5)	0.0043(6)	0.08371(11)	0.0134(10)	18
In2	6*c*	0.733(7)	0.6667	0.3333	-0.0018(7)	0.021(4)	6
In3	3*a*	0.534(14)	0.0000	0.0000	0.0000	0.043(11)	3

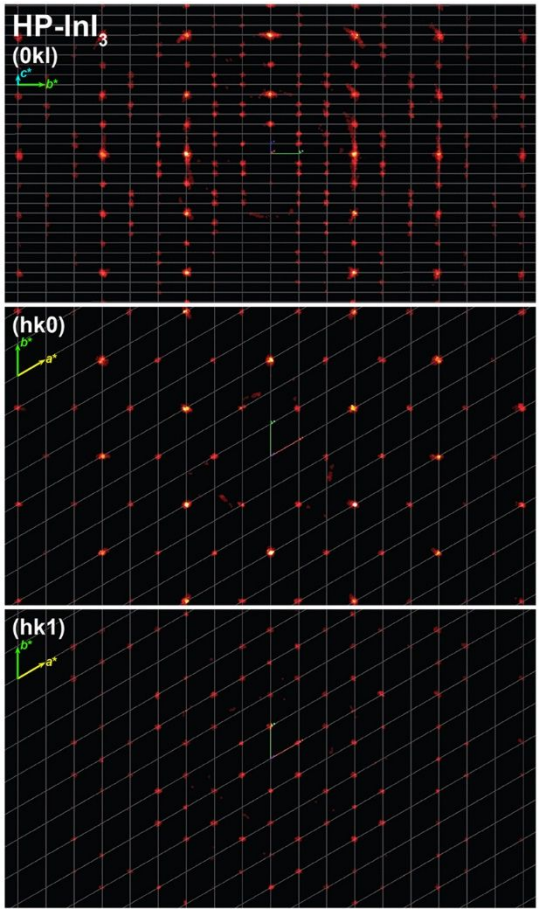

Figure 2 The 0kl (top) hk0 (middle) and hk1 (bottom) reciprocal lattice planes of single crystal HP-InI3 at 300 K.

transform to monoclinic AP-InI_3 under light radiation, or by heating with a transition temperature ranging from 23 to 69 °C. Our observations confirm that HP-InI_3 is metastable, and that the samples may undergo a partial phase transition due to a delicate stimulus from the environment. However, it was also observed that with good protection, an HP-InI_3 sample was unchanged in either color or structure under ordinary room light at room temperature in a N_2-protected glove box. This could be because a longer time, stronger light intensity, or higher energy radiation is needed to trigger HP-InI_3 to transform into the AP-phase than is needed for the low temperature form of InI_3. Another possible explanation is that an external factor (for example a tiny amount of moisture) might be needed to accelerate the phase transition. (This phenomenon has been observed in some halide systems, one instance being that $CsPbI_3$ was reported to catalytically transfer from a perovskite phase to a non-perovskite phase in the presence of moisture[25].) Diffuse reflectance measurements were conducted on both AP-InI_3 and HP-InI_3. Due to the metastability of the HP-phase, however, the measured sample might have partially transformed to the ambient pressure phase during the measurement and thus two transitions can be observed in the HP-InI_3 sample reflectance curve (Figure 3). According to the comparison of the two reflectance curves, and the correlation with their sample colors, we attribute the absorption between 500 to 600 nm to the HP-InI_3 phase, and a second absorption at around 400 nm to the AP-phase. The band gaps were calculated

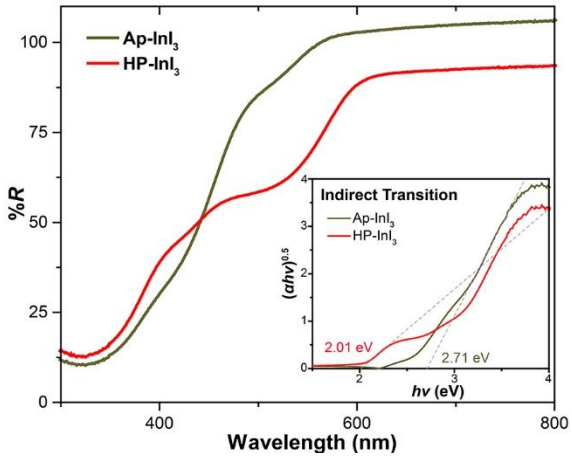

Figure3 Diffuse reflectance spectra of AP-InI_3 and HP-InI_3 samples. The inset presents the Tauc plots of indirect transitions to estimate the band gap values.

using Tauc plots (Figure 3 inset) based on the equation:[26] $(\alpha h\nu)^n = A\,(h\nu - E_g)$, where A is a constant and α is the absorption coefficient (cm^{-1}). (n is 2 for direct transitions, and 0.5 for indirect transitions.) For indirect transitions, the values of the band gaps are calculated to be 2.71(5) eV for AP-InI_3, and 2.01(2) eV for HP-InI_3. DFT calculations obtained from the Open Quantum Materials Database (OQMD) provide calculated density of states for both $R\bar{3}$ structure InI_3 and $P2_1/c$ structure InI_3 [27,28]. Based on that information, $R\bar{3}$ InI_3 has a calculated band gap of around 1.8 eV, while $P2_1/c$ InI_3 is calculated to have a band gap of 2.2 eV. Although it has been suggested that the band gaps estimated from diffuse reflectance using the Tauc plot may be usually underestimated[29], the larger band gap value of the monoclinic phase compared to the rhombohedral phase matches the experimental results.

The magnetic susceptibility (M/H) was measured versus increasing temperature on an HP-InI_3 powder sample under 1000 Oe. As is shown in the inset of Figure 4, temperature-independent diamagnetic behavior is revealed, which is in line with the expectation of the electron configuration of In(III). Heat capacity measurements were also conducted from 2 to 200 K on dense HP-InI_3 sample pieces. As presented in Figure 4's main panel, no sharp transitions are observed, consistent with the magnetization behavior of the sample. Some small slope variation can be observed on the curve, which looks similar to

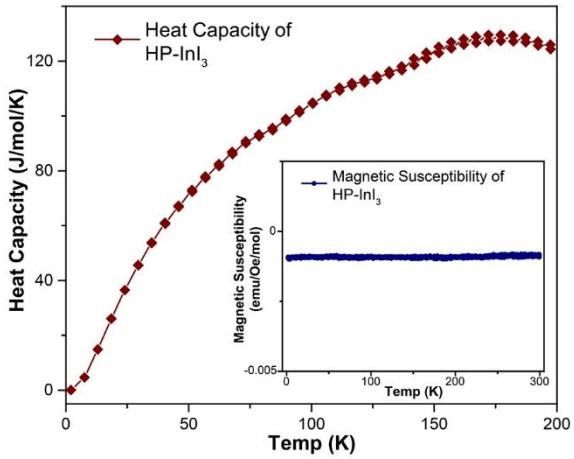

Figure 4 Magnetic susceptibility (inset) and heat capacity (main panel) data of HP-InI_3, plotted versus temperature.

what might happen for a second-order phase transition. A transition at around 93 K has been mentioned in previous reports[20]. These phase transitions may be due to a minor structural transformation, suggesting that more complex polymorphic behavior may be found in the indium iodine system than is presently known. Thus it may be of future research interest to determine the low temperature crystal structure of HP-InI_3.

Conclusions

A high-pressure stabilized InI_3 polymorph was obtained by a high-pressure high-temperature synthetic method. Its rhombohedral structure and $R\overline{3}$ unit cell have been determined by SCXRD and Rietveld refinement of PXRD data. The orange color and honeycomb layered structure distinguish this HP-phase from monoclinic AP-InI_3. Diffuse reflectance measurements are also conducted, from which the band gap values are estimated to be 2.71 eV for AP-InI_3 and 2.01 eV for HP-InI_3, for indirect transitions. Magnetization and heat capacity have also been characterized, and suggest that further study of the polymorphic behavior of the indium iodine system may be of future interest. Compared with the description in previous reports, high pressure plays a crucial role in synthesis and forces the structure towards layered honeycomb InI_3, which further confirms the potential of high-pressure synthesis in exploring and developing new solid-state materials.

Acknowledgements

This work was funded in large part by the Gordon and Betty Moore foundation, EPiQS initiative, grant GBMF-9066. The SCXRD work performed in Weiwei Xie's group was supported by the U.S. DOE-BES under Contract DE-SC0022156.

Author Contributions

Danrui Ni: Conceptualization, Methodology, Investigation, Formal analysis, Visualization, Writing - Original Draft; **Haozhe Wang**: Validation, Investigation, Formal analysis, Visualization, Writing - Reviewing and Editing; **Xianghan Xu:** Validation, Formal analysis, Visualization, Software, Writing - Reviewing and Editing; **Weiwei Xie**: Data curation, Resource, Supervision, Writing - Reviewing and Editing; **Robert J. Cava***: Conceptualization, Resource, Supervision, Project Funding acquisition, administration, Writing- Reviewing and Editing.

Conflicts of interest

The authors declare that they have no known competing financial interests or personal relationships that could have appeared to influence the work reported in this paper.

References

1 J. V. Badding, *Annu. Rev. Mater. Sci.*, 1998, **28**, 631–658.
2 D. A. Polvani, J. F. Meng, N. V. Chandra Shekar, J. Sharp and J. V. Badding, *Chem. Mater.*, 2001, **13**, 2068–2071.
3 B. Lorenz and C. W. Chu, in *Frontiers in Superconducting Materials*, ed. A. V. Narlikar, Springer, Berlin, Heidelberg, 2005, pp. 459–497.
4 Y. Shirako, X. Wang, Y. Tsujimoto, K. Tanaka, Y. Guo, Y. Matsushita, Y. Nemoto, Y. Katsuya, Y. Shi, D. Mori, H. Kojitani, K. Yamaura, Y. Inaguma and M. Akaogi, *Inorg. Chem.*, 2014, **53**, 11616–11625.
5 F. O. von Rohr, H. Ji, F. A. Cevallos, T. Gao, N. P. Ong and R. J. Cava, *J. Am. Chem. Soc.*, 2017, **139**, 2771–2777.
6 K. Nawa, Y. Imai, Y. Yamaji, H. Fujihara, W. Yamada, R. Takahashi, T. Hiraoka, M. Hagihala, S. Torii, T. Aoyama, T. Ohashi, Y. Shimizu, H. Gotou, M. Itoh, K. Ohgushi and T. J. Sato, *J. Phys. Soc. Jpn.*, 2021, **90**, 123703.
7 D. Ni, S. Guo, Z. S. Yang, K. M. Powderly and R. J. Cava, *Solid State Sciences*, 2019, **91**, 49–53.
8 D. Ni, S. Guo, K. M. Powderly, R. Zhong and R. J. Cava, *Journal of Solid State Chemistry*, 2019, **280**, 120982.
9 D. Ni, X. Gui, B. Han, H. Wang, W. Xie, N. P. Ong and R. J. Cava, *Dalton Trans.*, 2022, **51**, 8688–8694.
10 H. Hillebrecht, T. Ludwig and G. Thiele, *Zeitschrift für anorganische und allgemeine Chemie*, 2004, **630**, 2199–2204.
11 A. Banerjee, J. Yan, J. Knolle, C. A. Bridges, M. B. Stone, M. D. Lumsden, D. G. Mandrus, D. A. Tennant, R. Moessner and S. E. Nagler, *Science*, 2017, **356**, 1055–1059.
12 T. Kong, K. Stolze, E. I. Timmons, J. Tao, D. Ni, S. Guo, Z. Yang, R. Prozorov and R. J. Cava, *Advanced Materials*, 2019, **31**, 1808074.
13 J. Angelkort, A. Schönleber and S. van Smaalen, *Journal of Solid State Chemistry*, 2009, **182**, 525–531.
14 M. A. McGuire, *Crystals*, 2017, **7**, 121.
15 J. R. Chamorro, T. M. McQueen and T. T. Tran, *Chem. Rev.*, 2021, **121**, 2898–2934.
16 D. Ni, K. P. Devlin, G. Cheng, X. Gui, W. Xie, N. Yao and R. J. Cava, *Journal of Solid State Chemistry*, 2022, **312**, 123240.
17 Y. Imai, K. Nawa, Y. Shimizu, W. Yamada, H. Fujihara, T. Aoyama, R. Takahashi, D. Okuyama, T. Ohashi, M. Hagihala, S. Torii, D. Morikawa, M. Terauchi, T. Kawamata, M. Kato, H. Gotou, M. Itoh, T. J. Sato and K. Ohgushi, *Phys. Rev. B*, 2022, **105**, L041112.
18 D. Ni, X. Gui, K. M. Powderly and R. J. Cava, *Advanced Materials*, 2022, **34**, 2106831.
19 D. Ni, R. S. D. Mudiyanselage, X. Xu, J. Mun, Y. Zhu, W. Xie and R. J. Cava, *Phys. Rev. Mater.*, 2022, **6**, 124001.
20 P. P. Fedorov, A. I. Popov and R. L. Simoneaux, *Russ. Chem. Rev.*, 2017, **86**, 240.
21 J. D. Forrester, A. Zalkin and D. H. Templeton, *Inorg. Chem.*, 1964, **3**, 63–67.
22 F. Ensslin and H. Dreyer, *Zeitschrift für anorganische und allgemeine Chemie*, 1942, **249**, 119–132.
23 A. Liang, R. Turnbull, C. Popescu, F. J. Manjón, E. Bandiello, P. Rodriguez-Hernandez, A. Muñoz, I. Yousef, Z. Hebboul and D. Errandonea, *Phys. Rev. B*, 2022, **105**, 054105.
24 R. Kniep and P. Blees, *Angewandte Chemie International Edition in English*, 1984, **23**, 799–800.
25 D. B. Straus, S. Guo and R. J. Cava, *J. Am. Chem. Soc.*, 2019, **141**, 11435–11439.
26 J. Tauc, *Materials Research Bulletin*, 1968, **3**, 37–46.
27 J. E. Saal, S. Kirklin, M. Aykol, B. Meredig and C. Wolverton, *JOM*, 2013, **65**, 1501–1509.
28 S. Kirklin, J. E. Saal, B. Meredig, A. Thompson, J. W. Doak, M. Aykol, S. Rühl and C. Wolverton, *npj Comput Mater*, 2015, **1**, 1–15.
29 A. B. Garg, D. Vie, P. Rodriguez-Hernandez, A. Muñoz, A. Segura and D. Errandonea, *J. Phys. Chem. Lett.*, 2023, **14**, 1762–1768.